DOI: 10.1002/chem.200902320

Direct Growth of Single-Crystal Pt Nanowires on Sn@CNT Nanocable: 3D Electrodes for Highly Active Electrocatalysts

Shuhui Sun,[a] Gaixia Zhang,[a] Dongsheng Geng,[a] Yougui Chen,[a] Mohammad Norouzi Banis,[a] Ruying Li,[a] Mei Cai,[b] and Xueliang Sun*[a]

Abstract: A newly designed and fabricated novel three dimensional (3D) nanocomposite composed of single-crystal Pt nanowires (PtNW) and a coaxial nanocable support consisting of a tin nanowire and a carbon nanotube (Sn@CNT) is reported. This nanocomposite is fabricated by the synthesis of Sn@CNT nanocables by means of a thermal evaporation method, followed by the direct growth with PtNWs through a facile aqueous solution approach at room temperature. Electrochemical measurements demonstrate that the PtNW–Sn@CNT 3D electrode exhibits enhanced electrocatalytic performance in oxygen reduction reaction (ORR) for polymer electrolyte membrane fuel cells (PEMFCs), methanol oxidation (MOR) for direct methanol fuel cells (DMFCs), and CO tolerance compared with commercial ETEK Pt/C catalyst made of Pt nanoparticles.

Keywords: electrochemistry · fuel cells · nanomaterials · nanowires · platinum

Introduction

Platinum is the key electrocatalyst in polymer electrolyte membrane (PEM) fuel cells,[1–3] where it catalyzes oxygen reduction reaction (ORR) at the cathode and fuel (including hydrogen and methanol) oxidation reaction at the anode.[4,5] Interestingly, it has been established that the catalytic reactivity of Pt nanostructures depends highly on their morphology (including dimensionality and shape), and therefore the design and synthesis of well-controlled shapes and sizes of Pt nanostructures is crucial for their applications, especially in the field of electrocatalysis for fuel cells.[6,7]

To date, considerable efforts have been devoted to the synthesis of Pt nanostructures; however, most of these studies focused on spherical nanoparticles or nanoparticles with an undetermined shape.[8–10] Very recently, one dimensional (1D) Pt structures, such as nanowires, have drawn much attention owing to their unique anisotropic structure and surface properties, as well as excellent electrocatalytic activities.[11–14] Platinum nanowires have been synthesized by templating against the channels of hard or soft templates, however, polycrystalline nanowires were normally obtained.[15] The first attempt to generate single-crystal Pt nanowires was accomplished by Xia and coworkers through a polyol process, combined with the introduction of a trace amount of iron species; poly(vinyl pyrrolidone) was used as a surfactant, and the reaction was carried out at 110 °C.[11] It still remains a grand challenge to synthesize single-crystalline Pt nanowires through surfactant-free routes under mild conditions.

To improve the Pt utilization and enhance their catalytic activity, Pt catalysts are often dispersed onto a variety of carbon supports, including carbon black (CB),[16] carbon nanofibers (CNFs),[17] and carbon nanotubes (CNTs).[18] Among these supporting materials, CNTs are considered to be one of the most attractive candidates, owing to their outstanding mechanical characteristics, such as high tensile strength coupled with high surface area, high electric conductivity, and thermal conductivity.[19–20] Indeed, CNTs supported Pt nanoparticles showed enhanced ORR and methanol oxidation (MOR) activities in fuel cells.[21–24] Moreover, the addition of tin (Sn) or its oxide to Pt/CNT catalysts can further enhance their performance according to the bi-func-

[a] Dr. S. Sun, Dr. G. Zhang, Dr. D. Geng, Y. Chen, M. N. Banis, R. Li, Prof. X. Sun
Department of Mechanical and Materials Engineering
The University of Western Ontario
London, Ontario, N6A 5B9 (Canada)
Fax: (+1) 519-661-3020
E-mail: xsun@eng.uwo.ca

[b] Dr. M. Cai
General Motors Research and Development Center
Michigan 48090-9055 (USA)

Supporting information for this article is available on the WWW under http://dx.doi.org/10.1002/chem.200902320.

tional mechanism.[25–27] Despite the progress made in the past, the production of Pt catalyst with great catalytic performance and utilization efficiency is still costly and far from being trivial.

In this study, through a facile surfactant-free aqueous solution method, we synthesized ultrathin single-crystal Pt nanowires, at room temperature, on a Sn@CNT nanocable support directly grown on carbon paper fuel cell backing to form a novel 3D fuel-cell electrode (PtNW–Sn@CNT). Such a Sn@CNT 3D nanocable support holds many advantages, including enhancing effect of tin, higher gas permeability, improved metal-support interactions, and enhanced mass transport. This approach allows us to combine the advantages of both a PtNW catalyst and a Sn@CNT 3D nanocable support for fuel cell applications. The PtNW–Sn@CNT 3D electrodes showed greatly enhanced electrocatalytic activities for oxygen reduction, methanol oxidation and improved CO tolerance than commercial ETEK Pt/C catalyst made of Pt nanoparticles.

Results and Discussion

The approach and schematic illustration for the synthesis of Pt nanowires on Sn@CNT nanocable supports is demonstrated in Scheme 1. The actual synthetic procedure is very simple, and only two chemicals (H_2PtCl_6 and HCOOH) were used throughout the whole synthesis process, which did not require a stabilizing agent. Further, the reaction was conducted at room temperature in environmentally friendly aqueous solution.

Typical scanning electron microscopy (SEM) and transmission electron microscopy (TEM) images of the pristine Sn@CNT nanostructures grown on a commercially-available carbon paper fuel cell backing are shown in Figure 1. The carbon paper substrate is made of many graphite fibers with a diameter between 5 and 10 μm. As shown in Figure 1a and inset, after the growth of Sn@CNT, the surface of carbon fibers was completely covered with dense rod-like structures, approximately 5–10 μm in length and 150–200 nm in diameter. The TEM image of a coaxially integrated nanocable structure that consists of a Sn core and CNT shell with void space between the two is shown in Figure 1b. The carbon shell is about 60 nm thick and the diameter of the Sn core is about 70 nm. Energy dispersive X-ray spectroscopy (EDS) and selected area electron diffraction (SAED) of the core-shell structure confirmed the presence of metallic Sn and amorphous carbon.[28] The less graphitic form of carbon could promote H^+ diffusion into the Sn core through the "gaps" in the carbon shell.[29]

Typical SEM images of the PtNWs grown on Sn@CNT nanocables, at two magnifications, are shown in Figure 2a and b, respectively. They reveal that, after the complete surface coverage with hundred-nanometer long PtNWs, the Sn@CNT nanocables still maintain their "free-standing" 3D structures. The TEM image (Figure 2c, and Figure S1) further confirms the SEM investigation, showing that PtNWs

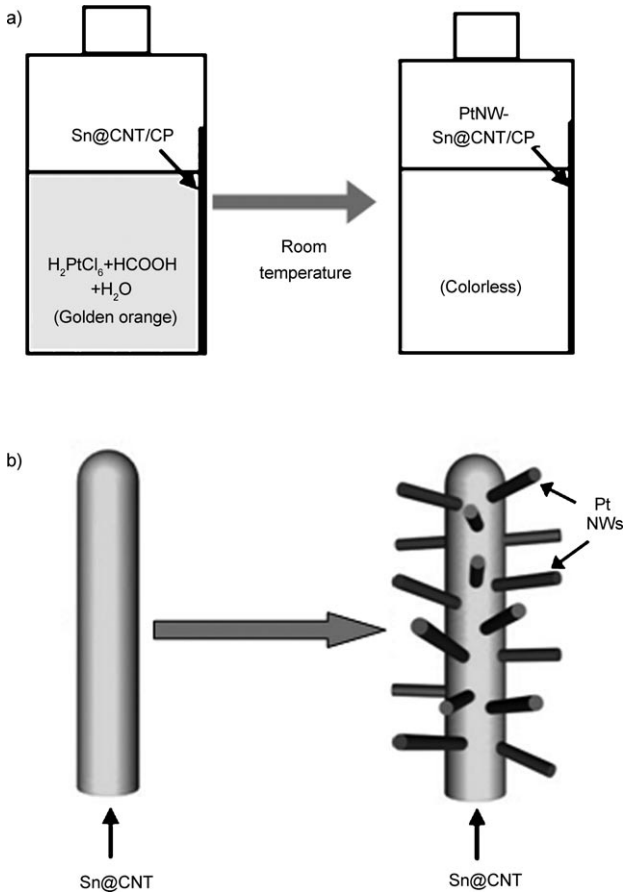

Scheme 1. a) Schematic representation of the approach in the synthesis of PtNW–Sn@CNT nanocomposites. b) Schematic image depicting the growth of PtNWs on Sn@CNT nanocable support.

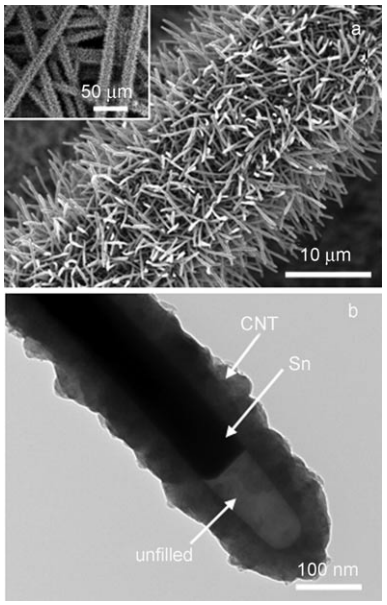

Figure 1. a) SEM and b) TEM images of pristine Sn@CNT nanocables, before the growth of Pt NWs.

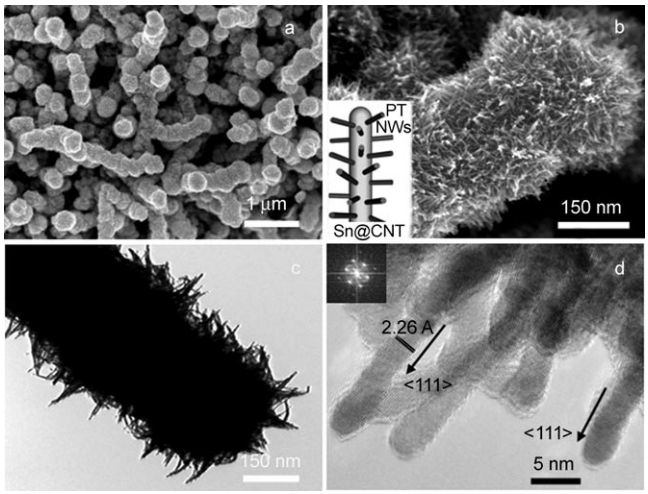

Figure 2. a) SEM, b) HRSEM, and c) TEM images of PtNW–Sn@CNT heterostructures, d) HRTEM image of Pt NWs grown on Sn@CNT nanocables.

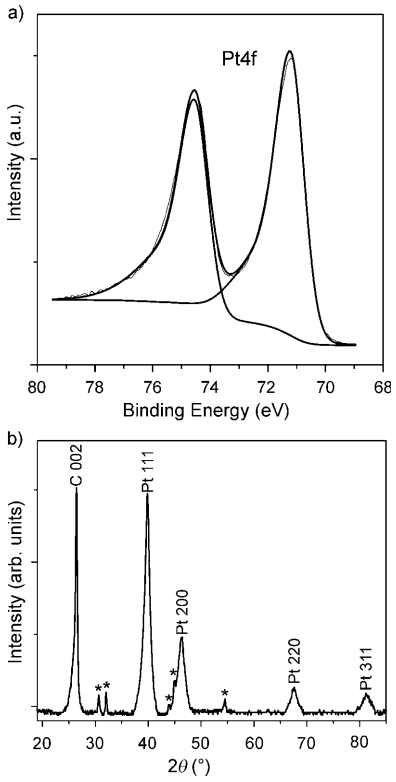

Figure 3. a) Pt4f XPS spectrum separation, and b) XRD patterns of Pt NWs grown on Sn@CNT nanocables. The * in b) represents the XRD patterns originated from Sn.

grow uniformly over Sn@CNT surface with lengths of up to hundred nanometers. High-resolution (HR) TEM examination (Figure 2d) shows that the Pt nanowires are ≈4 nm in diameter and they grow along the ⟨111⟩ direction. The crystallographic alignment of nanowires reveals that the entire nanowire is one single crystal with a lattice spacing between the {111} planes of 0.226 nm, which is in agreement with the value of bulk Pt crystal.[12] The fast Fourier transform (FFT) of the atomic-lattice fringing, apparent in the inset of Figure 2d, further confirms the single crystallinity of Pt nanowires.

The chemical state of PtNWs growth on Sn@CNT nanocable supports were determined by X-ray photoelectron spectroscopy (XPS). High resolution Pt 4f spectrum was deconvoluted into asymmetric doublet (Figure 3a) peaks centered at 71.4 and 74.7 eV, which can be attributed to $Pt^0\ 4f_{7/2}$, and $Pt^0\ 4f_{5/2}$, respectively. These are in good agreement with those of pure bulk platinum.[30] In addition, no obvious shoulders at higher binding energies, representing Pt^{2+} and Pt^{4+}, were found. Based on these analyses, we believe that the Pt NWs grown on Sn@CNT nanocable supports are pure metallic Pt. The X-ray diffraction (XRD) pattern, shown in Figure 3b, reveals that the Pt nanowires grown on Sn@CNT nanocable 3D supports were crystallized in a face-centered-cubic (fcc) structure similar to bulk Pt, which is consistent with the HRTEM investigations.

We believe that the growth of PtNWs on Sn@CNT supports follows the similar process to that for Pt NWs on MWCNTs.[12b] Typically, Pt nuclei are first formed in solution through the reduction of H_2PtCl_6 by HCOOH, and they deposit on the surface of Sn@CNT nanocables. The freshly formed nuclei act as the sites for further nucleation, through the continually absorption of Pt^{4+} ions, leading to the formation of clustered particles. As the reaction is conducted at room temperature, the reduction rate is very slow, and the anisotropic growth is favored because, for fcc structures, the order of surface energies is $(111)<(100)<(110)$.[12a] Therefore, according to the lowest energy principle, the growth rate along the closed-packed ⟨111⟩ direction is enhanced. We believe that the key to synthesize the Pt nanowires is to reduce the rate of Pt ion reduction, favoring the growth of {111} planes, and therefore leading to the formation of 1D nanowires.

We evaluated the electrochemical properties of the PtNW–Sn@CNT composite and, for comparison, pristine Sn@CNT nanocable structures and 30 wt% Pt/C (ETEK) catalysts, using cyclic voltammetry (CV). The CVs recorded between −0.25 and 0.95 V vs SCE in a deaerated 0.5 M H_2SO_4 solution are shown in Figure 4. Before Pt deposition, only background currents representing characteristic of carbon electrodes, are observed (solid line a). After the growth of Pt nanowires, clear and characteristic Pt surface electrochemistry is observed (solid line b), with hydrogen adsorption and desorption between 0.05 and −0.25 V, and Pt oxidation in the range of 0.55 to 0.95 V with reduction peak at 0.59 V. Multiple peaks for hydrogen adsorption and desorption, rather than a single broad peak, were observed, indicating that the reaction involved multiple exposed Pt crystallographic planes. The electrochemically active surface areas (ECSA) of the samples were calculated based on the

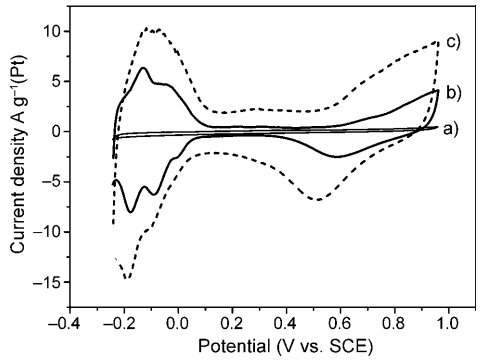

Figure 4. Cyclic voltammograms of a) pristine Sn@CNT; b) PtNW–Sn@CNT; and c) 30 wt% Pt/C commercial catalysts (ETEK). Measured at a scan rate of 50 mV s^{-1} in degassed 0.5 M H_2SO_4.

hydrogen adsorption wave capacity (Q_H) according to the following [Eqn. (1)]:[24]

$$A_{EL} = Q_H/(210\,\mu C\,cm^{-2} \times \text{Pt loading}) \quad (1)$$

The obtained value of A_{EL} for the PtNW–Sn@CNT is 17.2 $m^2\,g^{-1}$(Pt), which is 50% of that for the ETEK Pt/C catalyst [34.5 $m^2\,g^{-1}$(Pt)] made of Pt nanoparticles on carbon black (CB). This can be attributed to the intrinsic 1D morphology of nanowires compared to that of nanoparticles.[14]

The ORR activities of PtNW–Sn@CNT composite electrode and commercial Pt/C catalyst (ETEK) are shown in Figure 5. Both CVs were obtained in an O_2-saturated aqueous electrolyte solution containing 0.5 M H_2SO_4. It can be seen that a 60 mV positive shift of the onset potential for oxygen reduction at the PtNW–Sn@CNT composite was observed as compared to commercial Pt/C electrode. The oxygen reduction peak current, normalized on the basis of Pt loading, is 10.9 A g^{-1}(Pt) for the PtNW–Sn@CNT composite, which is 1.2 times that for the ETEK Pt/C catalyst [9.0 A g^{-1}(Pt)]. Interestingly, this improvement occurred in spite of a 50% lower Pt active surface area for the Pt nanowire catalyst. Taking into account both effects, a specific ORR activity for PtNW–Sn@CNT of 0.63 A m^{-2}(Pt) was obtained, which is 2.4 times better than for the ETEK Pt/C catalyst [0.26 A m^{-2}(Pt)]. The higher specific activity of the PtNW–Sn@CNT as compared to Pt nanoparticles on CB (ETEK) might be owed to the preferential exposure of certain crystal facets of the Pt NWs,[14,31] and/or the unique 3D structure of Sn@CNT-based electrode, which facilitates the O_2 diffusion to Pt surface. These results indicate a significant improvement of electrocatalytic activity for ORR in PtNW–Sn@CNT composite.

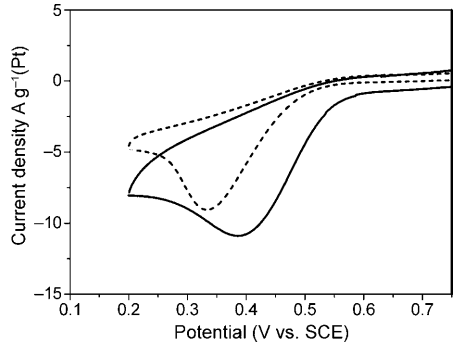

Figure 5. CVs for oxygen reduction reaction in O-saturated 0.5 M H_2SO_4 at PtNW–Sn@CNT (——) and commercial Pt/C electrode (ETEK) (-----). Potential scan rate 50 mV s^{-1}

The electrocatalytic activity of the PtNW–Sn@CNT composite for methanol oxidation, which is the heart of direct methanol fuel cell (DMFC) application in the anodic half-cell reaction, was also demonstrated by using a well-used electrochemical reaction in a solution containing 1 M MeOH and 0.5 M H_2SO_4. For comparison, the pristine Sn@CNT and the commercial ETEK Pt/C catalyst (30 wt% Pt) were also tested under the same experimental conditions. From the voltammograms shown in Figure 6, no obvious oxidation peaks could be observed from the CV curve of the pristine Sn@CNT electrode, indicating the support itself is catalytically inactive for methanol oxidation (curve a). Two typical oxidation peaks appear for the CV curves of the PtNW–Sn@CNT (curve b) and Pt/C catalysts (curve c), which arise from the oxidations of methanol and their intermediates.[32] Obviously, the peak potential for methanol oxidation in the forward scan on PtNW–Sn@CNT composite (0.66 V vs. SCE) is much lower than that (0.70 V vs. SCE) for Pt/C catalyst. This indicates that the PtNWs supported on Sn@CNT nanocables are able to significantly reduce the overpotential in methanol oxidation. The methanol oxidation peak current, normalized on the basis of Pt loading, for PtNW–Sn@CNT is about 91.0 A g^{-1}(Pt), which is 1.35 times higher than for the ETEK Pt/C catalyst [66.9 A g^{-1}(Pt)]. In terms of the activity per unit active surface area, ≈2.8 times higher specific activity for PtNW–Sn@CNT composite [5.3 A m^{-2}(Pt)] than that for the ETEK Pt/C [1.9 A m^{-2}(Pt)] were obtained. Goodenough et al. suggested the anodic peak in the reverse scan might be attributed to the removal of the incomplete oxidized carbonaceous species, such as

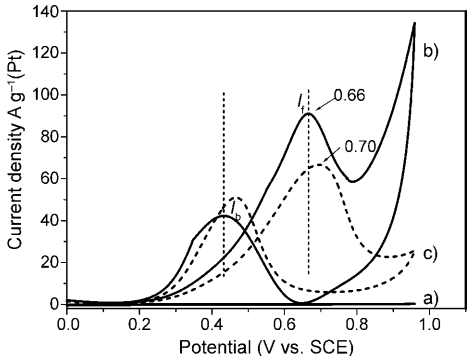

Figure 6. Cyclic voltammograms for methanol oxidation (1 M methanol in 0.5 M H_2SO_4). Trace a) before growth of PtNWs; trace b) after growth of PtNWs on Sn@CNT; trace c) ETEK commercial catalyst of Pt nanoparticles on carbon black.

CO, $HCOO^-$ and HCO^-, accumulated on catalyst surface during the forward scan. Consequently, the ratio of current densities for these two anodic peaks, I_f/I_b, can be used to infer the CO tolerance of the catalyst.[33] The low I_f/I_b value usually indicates poor oxidation of methanol to CO_2 during the forward anodic scan and excessive accumulation of residual carbon species on catalyst surface. On the other hand, a higher I_f/I_b ratio is indicative of improved CO tolerance. In our study, the observation of a much higher I_f/I_b value on PtNW–Sn@CNT composite (2.2 vs. 1.3 on ETEK Pt/C) suggests that methanol molecules can be more effectively oxidized on PtNW–Sn@CNT during the forward scan, generating relatively less poisoning species as compared to commercial Pt/C catalyst, indicating the better CO tolerance. To further explore the observed enhancement of CO tolerance, we carried out a CO electrostripping experiment. From Figure 7, we can see, for both catalysts, that a sharp peak appears during the first scan (solid line) and disappears in the subsequent scan (dash line), indicating that the adsorbed CO is completely oxidized during the first forward scan. When comparing the onset potential and the peak potential for CO electro-oxidation, significant differences between the two catalysts can be observed. The onset potential of CO oxidation on PtNW–Sn@CNT composite is at 0.11 V (vs. SCE), which is about 290 mV lower than that on commercial Pt/C catalyst (0.4 V vs. SCE). Further, the oxidative CO-stripping peak potential centers at 0.62 V for the commercial Pt/C catalyst, whereas on PtNW–Sn@CNT, it is located at 0.55 V. The significant negative shifts for the onset and peak potentials of 290 mV and 70 mV, respectively, indicate that the adsorbed CO can be more easily removed from PtNW–Sn@CNT catalyst than from ETEK commercial Pt/C catalyst. All these results indicate that PtNW–Sn@CNT is much more tolerant to CO poisoning.

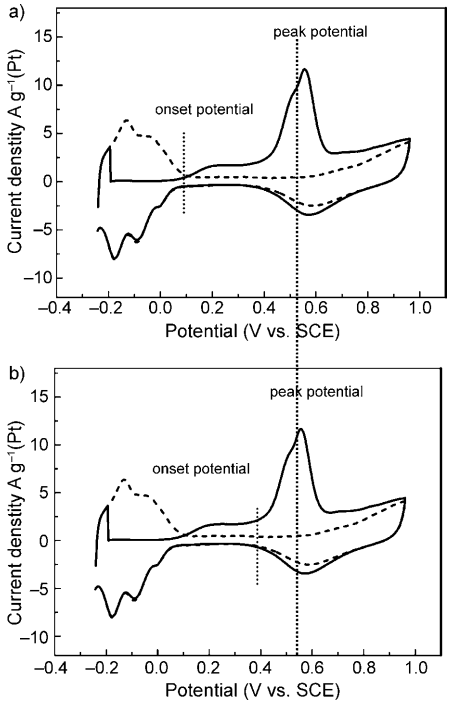

Figure 7. CVs of a) PtNW–Sn@CNT/carbon paper 3D electrode and b) a commercial Pt/C electrode in the presence of CO in 0.5 M H_2SO_4 aqueous solution at room temperature. Potential scan rate: 50 mV s.$^{-1}$ For both catalysts, a sharp peak appears during the first scan (solid line) and disappears in the subsequent scan (dash line).

As to the origin of the enhanced electrocatalytic performance on PtNW–Sn@CNT catalysts, several explanations can be suggested. In previous studies of Pt-based nanoparticle catalysts, the activity and CO tolerance enhancements were also observed on PtSn or $PtSnO_2$ nanostructures, which was attributed to the fact that tin (Sn) or its oxide could supply an oxygen containing (e.g. -OH groups) surface to remove strongly absorbed species like CO, according to a so-called bi-functional mechanism.[33–35] Therefore, the improved catalytic activity and CO tolerance observed in our study may originate partially from the unique core-shell nanocable supports containing a Sn core. In addition, the "free-standing" nanocable supports and Pt nanowires provide excellent electron conductivity, which might facilitate the reaction kinetics on the electrode surfaces, and improve the O_2 and methanol diffusion rate. Furthermore, the preferential exposure of certain crystal facets along with the less surface defects bearing characteristics of Pt nanowires promotes their catalytic activities.[14] More importantly, the unique 1D anisotropic morphology of Pt nanostructures can improve mass transport and catalyst utilization for the electrocatalytic reactions. Recently, Sun et al.[14] found that Pt nanowires on carbon black showed much enhanced specific catalytic activity for oxygen reduction than those of the state-of-the-art Pt nanoparticle catalyst. Meanwhile, Chen et al[31] and Bi et al[36] reported that 1D Pt nanostructures exhibited improved both activity and stability for oxygen reduction and methanol oxidation, respectively. Based on these arguments, it is expected that by growing 1D Pt nanostructures on various metal oxide nanowire supports and forming 3D network structures, the full advantage of several combining factors can be taken. These factors include the enhanced performance of Pt nanowire catalyst, excellent properties of catalyst support, and enhanced mass transport. This approach may open new and exciting possibilities for further improving the performance of PEMFC and DMFC.

Conclusions

In summary, a facile aqueous solution procedure has been successfully developed to grow single-crystal Pt nanowires on Sn@CNT heterostructured nanocables at room temperature, forming a 3D nanocomposite electrode. The PtNW–Sn@CNT composite shows, for ORR, 1.2 times higher mass activity and 2.4-fold better specific activity, and for MOR, 1.35 times higher mass activity and 2.8-fold better specific activity, than those of the commercial catalyst made of Pt nanoparticles on carbon black. This novel structure has the potential to possess high Pt utilization, high activity, and

high durability for fuel cell applications. Further optimization of the dimensional control, the preparation and evaluation of membrane electrode assemblies based on PtNW–Sn@CNT catalysts are underway. This simple and unique approach can be extended to grow Pt nanowires on other 1D nanostructures, such as CNT, SnO_2, WO_3, TiO_2 etc., for wider applications.

Experimental Section

Sn@CNT nanocables synthesis: The synthesis of Sn@CNT nanocable structures was carried out by a thermal evaporation method.[28] In a typical process, pure Sn powders (2 g, −325 mesh, 99.8%) were placed in an alumina boat located at the center of a quartz tube in a horizontal tube furnace. A small piece of commercially available carbon paper (ETEK, 0.17 mm thick, 81% porosity) was placed aside of the metal powder, acting as the substrate. The reaction chamber was first heated to 850°C rapidly (in about 15 min) from room temperature under an atmosphere of flowing Ar and 2% ethylene (200 sccm), and then kept at 850°C for 2 h. After the furnace was cooled down to room temperature, a gray dark thin film was observed on the surface of the carbon paper substrate.

Growth of Pt nanowires on Sn@CNT/carbon paper: The growth of Pt nanowires on Sn@CNT support was conducted by the chemical reduction of Pt precursor with formic acid.[12] In a typical procedure, 0.032 g hexachloroplatinic acid ($H_2PtCl_6{\cdot}6H_2O$, Aldrich) and 1 mL formic acid (HCOOH, Aldrich) were added simultaneously into 20 mL H_2O at room temperature to form a golden orange solution. The Sn@CNT/carbon paper was immersed into the solution, acting as the growth substrates, and then the reaction proceeded at room temperature without stirring for up to 3 days until the solution color gradually changed to colorless. After the completion of the reaction, PtNW–Sn@CNT/carbon paper was washed with deionized water and dried at 80°C over night in a vacuum oven. The Pt loading was determined to be 0.4136 mg cm^{-2} by using inductively coupled plasma-optical emission spectroscopy (ICP-OES) (the total amount of Pt divided by the geometric surface area of the composite electrode). The morphology of the prepared catalyst were characterized by using SEM (Hitachi S-5200) and TEM (JEOL 2100F).

Electrochemical measurements: The electrochemical properties of the PtNW–Sn@CNT/carbon paper composites were evaluated by using cyclic voltammetry (CV) in a standard three-electrode cell at room temperature. A Pt wire was used as the counter electrode and a saturated calomel electrode (SCE) was used as the reference. CV measurements were carried out by using an Autolab potentiostat/galvanostat (Model, PGSTAT-30, Ecochemie, Brinkman Instruments), using 0.5 M H_2SO_4 solution purged with N_2 at a sweep rate of 50 mV s^{-1}. The electrochemical surface areas (ECSA) of Pt were calculated from the hydrogen adsorption peak of the CV. For methanol oxidation reaction, the CVs were measured in an air-free aqueous solution containing 1 M MeOH and 0.5 M H_2SO_4. For CO stripping voltammetry, pure CO (99.5%) was purged into the solution at a position close to the working electrode for 1 h, with the electrode polarized at 0.05 V versus RHE in a fume hood. The electrode was then purged with pure Ar for 1 h under potential control followed by voltammetric stripping.

For comparison, a conventional electrode made with commercial 30 wt% Pt/C catalyst from ETEK (USA), was also evaluated. The electrode was prepared with a procedure similar to the one reported previously.[37] Typically, 10 mg catalyst was sonically mixed with 1 mL H_2O/isopropanol (1/1 in volume ratio) to make a suspension. GC disk electrodes (5 mm diameter, Pine Research Instrument) that serve as the support were polished to a mirror finish before using. 20 μL of catalyst suspension was pipetted onto the GC disk substrate, leading to a Pt loading of 0.3058 mg cm^{-2}, which is similar to that for PtNW–Sn@CNT composite electrode. The catalyst films were dried under flow N_2 at room temperature. Finally, a 10 μL Nafion (0.05 wt%) solution was pipetted onto the catalyst film, and then dried. The currents were normalized on the basis of Pt loading.

Acknowledgements

This research was supported by General Motors of Canada, Natural Sciences and Engineering Research Council of Canada, Canada Research Chair Program, Canada Foundation for Innovation, Ontario Early Researcher Award and the University of Western Ontario. S. Sun is grateful to the NSERC scholarship, and G. Zhang thanks the financial support from Ontario PDF Program. The authors thank Fred T. Wagner, General Motors, for his valuable advice on data analysis.

[1] E. Antolini, *Mater. Chem. Phys.* **2003**, *78*, 563.
[2] D. R. Rolison, *Science* **2003**, *299*, 1698.
[3] H. A. Gasteiger, S. S. Kocha, B. Sompalli, F. T. Wagner, *Appl. Catal. B* **2005**, *56*, 9.
[4] N. P. Brandon, S. Skinner, B. C. H. Steele, *Annu. Rev. Mater. Res.* **2003**, *33*, 183.
[5] R. K. Rao, D. C. Trivedi, *Coord. Chem. Rev.* **2005**, *249*, 613.
[6] J. Chen, T. Herricks, Y. Xia, *Angew. Chem.* **2005**, *117*, 2645; *Angew. Chem. Int. Ed.* **2005**, *44*, 2589.
[7] H. Lee, S. E. Habas, S. Kweskin, D. Butcher, G. A. Somorjai, P. Yang, *Angew. Chem.* **2006**, *118*, 7988; *Angew. Chem. Int. Ed.* **2006**, *45*, 7824.
[8] F. Mirkhalaf, J. Paprotny, D. J. Schiffrin, *J. Am. Chem. Soc.* **2006**, *128*, 7400.
[9] T. S. Ahmadi, Z. Wang, T. C. Greem, A. Heglein, M. A. El-Sayed, *Science* **1996**, *272*, 1924.
[10] H. Bönnemann, K. S. Nagabhushana, *J. New Mater. Electrochem. Syst.* **2004**, *7*, 93.
[11] J. Chen, T. Herricks, M. Geissler, Y. Xia, *J. Am. Chem. Soc.* **2004**, *126*, 10854.
[12] a) S. Sun, D. Yang, D. Villers, G. Zhang, E. Sacher, J. P. Dodelet, *Adv. Mater.* **2008**, *20*, 571; b) S. Sun, D. Yang, G. Zhang, E. Sacher, J. P. Dodelet, *Chem. Mater.* **2007**, *19*, 6376.
[13] E. P. Lee, Z. Peng, W. Chen, S. Chen, H. Yang, Y. Xia, *ACS Nano* **2008**, *2*, 2167.
[14] S. Sun, F. Jaouen, J. P. Dodelet, *Adv. Mater.* **2008**, *20*, 3900.
[15] J. Chen, B. J. Wiley, Y. Xia, *Langmuir* **2007**, *23*, 4120.
[16] Z. Zhou, S. Wang, W. Zhou, G. Wang, L. Jiang, W. Li, S. Song, J. Liu, G. Sun, Q. Xin, *Chem. Commun.* **2003**, 394.
[17] J. Zheng, M. Wang, X. Zhang, Y. Wu, P. Li, X. Zhou, W. Yuan, *J. Power Sources* **2008**, *175*, 211.
[18] S. Guo, S. Dong, E. Wang, *J. Phys. Chem. C* **2008**, *112*, 2389.
[19] T. W. Ebbesen, H. J. Lezec, H. Hiura, J. W. Bennett, H. F. Ghaemi, T. Thio, *Nature* **1996**, *382*, 54.
[20] R. H. Baughman, A. A. Zakhidov, W. A. Heer, *Science* **2002**, *297*, 787.
[21] Y. Lin, X. Cui, C. Yen, C. M. Wai, *J. Phys. Chem. B* **2005**, *109*, 14410.
[22] Y. Xing, *J. Phys. Chem. B* **2004**, *108*, 19255.
[23] M. S. Saha, R. Li, X. Sun, *J. Power Sources* **2008**, *177*, 314.
[24] D. Villers, S. Sun, A. M. Serventi, J. P. Dodelet, *J. Phys. Chem. B* **2006**, *110*, 25916.
[25] X. Zhao, W. Li, L. Jiang, W. Zhou, Q. Xin, B. Yi, G. Sun, *Carbon* **2004**, **42**, 3251.
[26] C. Du, M. Chen, X. Cao, G. Yin, P. Shi, *Electrochem. Commun.* **2009**, *11*, 496.
[27] M. S. Saha, R. Li, M. Cai, X. Sun, *J. Powder Sources* **2008**, *185*, 1079.
[28] R. Li, X. Sun, Y. Zhou, M. Cai, X. Sun, *J. Phys. Chem. C* **2007**, *111*, 9130.
[29] Y. Wang, J. Y. Lee, *Angew. Chem.* **2006**, *118*, 7200; *Angew. Chem. Int. Ed.* **2006**, *45*, 7042.
[30] P. Marcus, C. Hinnen, *Surf. Sci.* **1997**, *392*, 134.
[31] Z. W. Chen, M. Waje, W. Li, Y. Yan, *Angew. Chem.* **2007**, *119*, 4138; *Angew. Chem. Int. Ed.* **2007**, *46*, 4060.
[32] G. Che, B. B. Lakshmi, E. R. Fisher, R. Martin, *Nature* **1998**, *393*, 346.
[33] R. Manohara, J. B. Goodenough, *J. Mater. Chem.* **1992**, *2*, 875.

[34] F. Colmati, E. Antolini, E. R. Gonzalez, *J. Power Sources* **2006**, *157*, 98.
[35] P. Bommersbach, M. Mohamedi, D. Guay, *J. Electrochem. Soc.* **2007**, *154*, B876.
[36] Y. Bi, G. Lu, *Electrochem. Commun.* **2008**, *10*, 45.
[37] M. Sudan Saha, R. Li, M. Cai, X. Sun, *Electrochem. Solid-State Lett.* **2007**, *10*, B130.

Received: August 22, 2009
Published online: December 18, 2009

